energies

IMPACT FACTOR 3.0

CITESCORE 6.2

Article

Model of a Hybrid Electric Vehicle Equipped with Solid Oxide Fuel Cells Powered by Biomethane

Giulia Sandrini, Marco Gadola, Daniel Chindamo and Laura Zecchi

MDPI

https://doi.org/10.3390/en16134918

energies

MDPI

Article

Model of a Hybrid Electric Vehicle Equipped with Solid Oxide Fuel Cells Powered by Biomethane

Giulia Sandrini [1,*], Marco Gadola [1], Daniel Chindamo [1] and Laura Zecchi [2]

[1] Department of Mechanical and Industrial Engineering, University of Brescia, I-25123 Brescia, Italy; marco.gadola@unibs.it (M.G.); daniel.chindamo@unibs.it (D.C.)
[2] Department of Information Engineering, University of Brescia, I-25123 Brescia, Italy; l.zecchi@unibs.it
* Correspondence: g.sandrini005@unibs.it

Abstract: To promote the development of new technologies that allow an intensive use of renewable green energies and to overcome the problem of the lack of range of full electric vehicles, an interesting energy source is biomethane. The Fuel Cells (FCs) systems benefit from high efficiency and zero emissions, and they are generally powered by hydrogen. One of the main problems related to hydrogen FCs is the current weak network of infrastructure's need to supply the hydrogen itself. An alternative may be the development of FC vehicles powered by methane, or biomethane, to exploit a renewable energy source. The type of Fuel Cells that lends itself to a methane (or biomethane) power supply is the Solid Oxide Fuel Cell (SOFC). Considering the limitations of the SOFCs, a vehicle model powered by Fuel Cells fueled by methane (or biomethane) is created. This work concerns the creation of a vehicle model, and the sizing of the SOFC system (generator delivering a constant 3 kW) and battery pack (30 Ah), for a door-to-door waste collection vehicle, whose mission is known. The latter is a fundamental requirement due to the limitations found for Solid Oxide Fuel Cells: slow transient and long ignition times.

Keywords: mathematical modeling; energy consumption; alternative propulsion; Solid Oxide Fuel Cell (SOFC); Fuel Cells powered by methane; vehicle model

Citation: Sandrini, G.; Gadola, M.; Chindamo, D.; Zecchi, L. Model of a Hybrid Electric Vehicle Equipped with Solid Oxide Fuel Cells Powered by Biomethane. *Energies* **2023**, *16*, 4918. https://doi.org/10.3390/en16134918

Academic Editor: Felix Barreras

Received: 5 June 2023
Revised: 19 June 2023
Accepted: 20 June 2023
Published: 24 June 2023

1. Introduction

To promote the development of new technologies that allow for an increasingly frequent and wide use of renewable green energies and that make it possible to overcome the problem of the lack of range of full electric vehicles, an interesting alternative energy source is biomethane.

An innovative vehicle power supply technology is the hydrogen Fuel Cell (FC) system, benefiting from high efficiency and zero emissions, provided that, by extending the analysis to the entire production process, the hydrogen necessary for its operation is obtained using renewable energies. An alternative may be Fuel Cell vehicles powered by biomethane to exploit a renewable energy source and to use the methane supply infrastructure already present for internal combustion vehicles and not present for hydrogen.

Fuel cells are electrochemical devices capable of carrying out a direct conversion from chemical energy to electrical energy in the form of a direct current between two electrodes maintained at a constant potential difference [1]. One of the main advantages of their use is the possibility of carrying out the energy conversion while maintaining high efficiency [2], avoiding the irreversibility of combustion typical of thermodynamic cycles [3].

The type of Fuel Cells capable of running on methane (or biomethane) as a power supply is the so-called Solid Oxide Fuel Cell (SOFC). Furthermore, SOFC systems have higher efficiencies than other systems (diesel-powered systems, gas engine systems, steam systems, etc.) and SOFCs are also more efficient than several other types of Fuel Cells, including the PAFC (Phosphoric Acid Fuel Cell) and PEFC (Polymer Electrolyte Fuel Cell) [3].

The peculiar characteristic of Solid Oxide Fuel Cell (SOFC) systems is precisely that of being able to be fueled with fuels other than hydrogen [4,5], such as natural gas (remembering that natural gas is composed of approximately 90% methane), biogas, methane, bioethanol, and synthesis gas obtained from the reforming of high-molecular-weight hydrocarbons, including diesel, etc. All this occurs by means of the reforming process that takes place inside the SOFC itself and which allows hydrogen molecules to be obtained from different fuels.

Most natural gas-fired power plants currently in operation have efficiencies around 30%. The conversion of natural gas into Solid Oxide Fuel Cells promises an increase in system-wide conversion efficiencies of more than 60%, doubling the current efficiencies of traditional systems and significantly reducing CO_2 emissions by a factor of two [6]. It is therefore possible to exploit SOFC technology on vehicles to improve their efficiency, when compared to traditional internal combustion vehicles fueled by methane.

By means of a study of the state of the art of SOFC (Solid Oxide Fuel Cell) systems, it was possible to find the necessary information for the realization of a model equipped with an SOFC system fueled by methane (or biomethane). The aim of this paper was in fact to create a model of a Solid Oxide Fuel Cell vehicle, which could become functional and bring advantages [7], taking into account all the limitations and criticalities foreseen for the SOFCs. Furthermore, the SOFC model was also integrated into a model for the simulation of the longitudinal dynamics of electric and hybrid vehicles, also present in the literature [8], with features similar to those presented in Ref. [9].

On the other side, some limitations must be taken into account. The slow transient linked to the chemical reactions that take place inside them make the SOFCs unsuitable for use on vehicles as a primary energy source. The choice, therefore, necessarily fell on their use as a generator that charges the battery pack during the use of the vehicle. For this reason, vehicles operating in fleet are the best choice and are well suitable with this kind of FC. The study presented in this paper will in fact concern the construction of a vehicle model equipped with SOFCs, and the sizing of the FC itself and battery pack, for a waste collection vehicle, whose mission is known, which is therefore predefined.

Another important criticality of SOFCs is their fragility, which means that the work carried out in this area is suitable for any future studies and designs, which may involve a solution to this problem. The barrier of the fragility of Solid Oxide Fuel Cells must therefore be overcome before the actual realization of a vehicle with SOFCs on board.

Therefore, the creation of a hybrid vehicle having another energy source on board (SOFCs) in addition to the battery pack allows the latter to be sized with a lower capacity. This can be achieved by means of an energy optimization on board the vehicle, which allows for a reduction in consumption during normal operations (less weight on board) and to save resources in the production phase of the pack itself.

This paper will propose a vehicle model equipped with Solid Oxide Fuel Cells that could represent a future application of SOFC technology on board electric vehicles to exploit the high efficiency of the system, combined with the possibility of powering these vehicles with biomethane, which is theoretically considered to have net-zero CO_2 impact. In fact, the carbon dioxide that is released into the atmosphere by the Fuel Cell as a waste product, from a life cycle perspective, is already considered amortized by the entire production process of the biomethane itself. The impact given by this CO_2 is in fact inevitable, even in the event of not producing/using biomethane.

In Ref. [10], a hybrid SOFC/battery vehicle configuration is proposed. In particular, the SOFC system can either charge the battery pack or propel the vehicle. This last aspect complicates the system and, considering that SOFCs are characterized by slow transients, powering the traction motor directly would not guarantee particular advantages. Often, in fact, the SOFC system would not be able to satisfy the mission's power demand, characterized by rapid variations. Another problem of the system described in Ref. [10] is the slow start-up time. This aspect was solved in our work by assuming a vehicle configuration with an SOFC always active to be connected to the grid whenever the vehicle is off duty, thus avoiding overcharging the battery pack.

In Ref. [11], the work presented aims at the realization of potential technology for the SOFC system in the automotive sector. This article discusses "Battery Electric Vehicle Range Extension", but a model for the vehicle layout is not proposed. However, the power target of the SOFCs made for study [11] adapts to the vehicle model proposed here. Ref. [12] also presents automotive SOFC systems but does not feature any vehicle model with SOFCs on board. In fact, article [12] focuses mainly on a particular technique for controlling SOFCs and the implementation of a DC/DC converter model. Another article that refers to the use of SOFCs in the automotive field, but which in this regard does not report any vehicle model, is paper [13]. The latter is focused on the chemistry of SOFCs, in particular on the strategies that allow for an improvement of their electrochemical performance and, therefore, an increase in power density.

In Ref. [7] an SOFC model for the transportation sector is proposed. However, work [7] focuses on Fuel Cells powered by a mixture of hydrogen, water, carbon monoxide, and carbon dioxide gas, not considering a methane (or biomethane) power supply. Furthermore, the model produced relates only to the SOFC system; no vehicle model with SOFCs on board is mentioned. Conversely, in the work proposed in this paper, we focus on the vehicle model, in such a way as to make it possible, through the appropriate measures, to use the SOFC technology on board battery electric vehicles.

Paper [14] represents an interesting work on Solid Oxide Fuel Cells combined with gas turbines, used as a range extender in hybrid electric vehicles. The article focuses on the thermal aspects related to SOFC technology, an aspect which on the other hand, is postponed to future developments, regarding the work we propose.

In Ref. [15], two types of hybrid vehicles with Fuel Cells on board are presented: a hybrid vehicle equipped with Proton Exchange Membrane Fuel Cells (PEMFCs) and a hybrid vehicle equipped with a Solid Oxide Fuel Cell (SOFC) stack to be used as a range extender. The two powertrains, PEMFC and SOFC, were simulated on a WLTC standard driving cycle of the WLTP procedure [16]. In Ref. [15], however, the PEMFC and SOFC models are accurately described, but the vehicle model adopted for the simulations is not.

In the work proposed in this paper, a model is created for a specific hybrid vehicle operating in a fleet, equipped with an SOFC system and battery pack. The work can be useful as a guideline for the realization of similar models (hybrid electric vehicles equipped with an SOFC system) for vehicles that operate with a predefined mission, exploiting the same hypotheses identified for the construction of the waste collection vehicle.

This paper is organized as follows:

- In Section 2, the model of the hybrid electric vehicle equipped with an SOFC stack is described. The realization of the model was possible by means of the identification of the main characteristics of the SOFC systems and by means of the knowledge of the vehicle mission.
- In Section 3, the results of the simulations are presented, regarding the vehicle model on its standard missions.
- In Section 4, the results obtained in Section 3 are discussed.
- In Section 5, some concluding remarks and final considerations are given.

2. Materials and Methods

The aim of this paper is to create a vehicle model powered by biomethane (or methane), in which methane is not burned as with internal combustion engines, but which provides energy through the chemical reactions carried out by means of a Fuel Cell stack.

The vehicle layout is chosen considering the various limitations imposed by the SOFC technology; in particular, a hybrid configuration is chosen, where the electric traction motor is powered by the battery pack, which in turn is charged by an SOFC stack that acts as a generator delivering constant power.

The capacity of the battery pack and the power of the Fuel Cell are sized by means of simulations after integrating the vehicle model under examination within the TEST model described in scientific article [8]. In particular, the latest version of this tool is used,

which includes the possibility of activating a particular regenerative braking logic [17] and the possibility of simulating hybrid vehicles equipped with PEMFCs (Proton Exchange Membrane Fuel Cells) [18].

2.1. Characteristics and limitations of SOFC Systems

As anticipated, the type of Fuel Cell that can be fueled by methane (or biomethane) is the Solid Oxide FC. Some useful information relating to SOFCs is summarized below, to be taken into account during modeling, commented to show how they interfaced with the biomethane Fuel Cell vehicle model.

- The SOFCs, through the reforming process, accept different possible feeds [4,5]: hydrogen, natural gas, biogas, methane, biomethane, bioethanol, diesel, etc. For this reason, this type of Fuel Cell is chosen for the vehicle model, so that the latter can be powered by biomethane (or methane).
- Undesirable characteristics of SOFCs are fragility and low vibration resistance. These limitations impose difficulties for use in the automotive sector [19]. The limit given by these characteristics must be overcome for the actual construction of a vehicle based on the model proposed in this work.
- SOFCs are characterized by high operating temperatures (500–1000 °C, depending on the type of SOFC) [10] and by different coefficients of thermal expansion. The fragility of SOFCs derives in part from this aspect [19]. Therefore, accurate thermal management is required on the vehicle subject of this study. Furthermore, having a component on the vehicle that operates at as little as 500 °C means that accurate thermal management is very important to ensure safety. It is also true that internal combustion engines typically reach temperatures above 1000 °C, but in this case, the high temperature is confined only to a small portion inside the cylinders, while the temperature already drops to around 100 °C in the vehicle's radiator.
- Solid Oxide FCs are characterized by slow transients (order of minutes). This makes them unsuitable for use on a vehicle as a primary energy source. Typically, vehicle missions are in fact characterized by rapid changes in power. For this reason, the vehicle model provides a configuration with purely electric traction, powered by a battery pack (which acts as a primary energy source) and an on-board SOFC stack that acts as a generator, charging the battery pack, consuming biomethane (or methane).
- Finally, SOFCs are also characterized by long start-up times [10] (order of hours). This aspect is related to the fact that the SOFC electrolytes have low ionic conductivity at low temperatures [20]. Therefore, long times are required for the preheating of the cells. To overcome this problem, once the new vehicle is put into operation and the FC is switched on, it is chosen to never switch off the SOFC. The methane-powered FC then recharges the battery pack during the vehicle operations and also when the vehicle is off if there is a need to raise the State of Charge of the batteries. By taking advantage of this charging method, the vehicle model is designed without the possibility of recharging the battery pack by connecting it to the electricity grid. Once the battery pack reaches the desired SOC (State of Charge), the vehicle must be connected to the stationary electrical network and the SOFC, which will always remain on, sends power to the grid.

2.2. Hypotheses Adopted for Model Construction

The following assumptions are made for the vehicle model object of this work, considering the SOFC characteristics and limitations exposed in the previous section.

- Use of a Solid Oxide FC stack (SOFC).
- Biomethane (or methane) power supply, assuming biomethane and methane are used with a comparable purity level, and therefore, being able to use the two power supplies (biomethane and methane) interchangeably.
- FC acts as a constant power generator to charge the battery pack.

- Fuel Cell is always active, even when the vehicle is off. The vehicle, for safety reasons, must in any case be equipped with an emergency system that can turn off the SOFC in the event that any problems occur, including the exceeding of a certain maximum SOC threshold of the battery pack during the vehicle's use phase.
- It is considered a vehicle that works in a fleet with a predefined mission, in particular, a door-to-door waste collection vehicle. In fact, a vehicle with a fixed mission allows for use of the above-mentioned configuration.
- During the inactivity phases, the vehicle must be connected to the electricity grid; in fact, once the battery pack reaches the desired SOC (State of Charge), the Fuel Cell sends power to the grid itself. Alternatively, it will be possible to charge other vehicles in the fleet (for example, full electric vehicles) or a stationary energy storage system.

2.3. Vehicle

The vehicle considered for the study is a vehicle operating in fleet for door-to-door waste collection, the same vehicle used for the low-performance validation of the TEST model, as described in Ref. [8]. The main data of the vehicle are reported in Table 1 in Ref. [8], while in Figure 5 in Ref. [8], the traction motor torque characteristics are shown.

However, some changes were made to the vehicle presented in Ref. [8]. The first change obviously relates to the SOFC system that was installed on the vehicle, a system which acts as a generator by charging the battery pack.

Another change concerns the total transmission ratio, set equal to 6.22, divided into a ratio of 3.11 for the motor reducer and equal to 2 for the rear differential (the vehicle is a rear-wheel drive). This is to allow the vehicle to reach the maximum speed required during its standard missions. Figure 1 shows the motor power and the power needed to overcome the resistance due to the aerodynamic force (drag) and the rolling resistance given by the interaction between tires and ground.

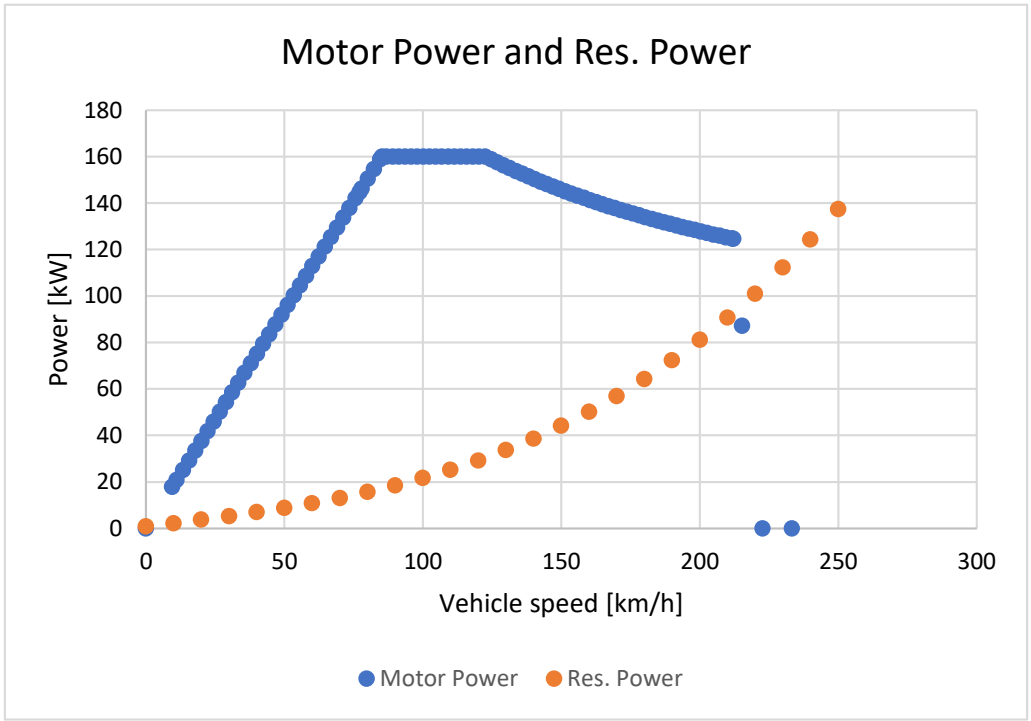

Figure 1. Maximum deliverable power of the electric traction motor (in blue) and sum of the resisting powers due to aerodynamic force and rolling resistance (in orange), as a function of the constant speed travelled by the vehicle. Assuming a total mass of the vehicle (including the transported load) equal to 3530 kg.

Another aspect that differentiates the simulations presented in Ref. [8] from the vehicle model object of this work is the mass. The simulations in this work are carried out with variable mass of the vehicle, as a function of time during the mission. In particular, the variable mass is associated with the payload carried during the use phase of the vehicle. First, the vehicle empty weight (including battery pack, Solid Oxide Fuel Cell, and tank with biomethane) equal to 1900 kg is considered. Furthermore, a constant driver mass equal to 80 kg and a variable mass relative to the payload carried by the vehicle during the speed profiles of the missions are considered. This last aspect will be explored in Section 2.4.

Finally, the last change concerns the battery pack (object of sizing, together with the Fuel Cell) and the size of the section of the electrical connection cables between the electric motor and the batteries. It is chosen to consider a hypothetical configuration and type of battery pack that allows it to deliver a current (discharge current) equal to a maximum of 360 Amps, and the object of the sizing is instead the capacity of the pack itself. Therefore, considering this limitation, the electric cables are dimensioned in such a way as to be able to withstand a maximum current of 360 A. For the cable's size, a maximum current density of 3.5 A/mm^2 is also considered as regards the cable itself. By dividing the maximum current of 360 A by the current density, a cable section of approximately 102.86 mm^2 is calculated, which corresponds to a cable diameter (circular section) of approximately 11.44 mm. To maintain safety, a conductor cable diameter of 12 mm is set for the simulations and for the model. During the construction of the prototype, the commercial section immediately above 102.8 mm^2 should be chosen, which corresponds to 120 mm^2 (diameter of 12.36 mm). It would therefore have been more appropriate to adopt a diameter of 12.36 mm in the model, but having approximated to 12 mm does not involve substantial differences in the results obtained.

2.4. Speed Profiles of Vehicle Missions

The mission of the door-to-door waste collection vehicle is known, as the daily speed profiles are acquired through a MoTeC data logger [21], a GPS receiver, and many other sensors installed on board the benchmark diesel-powered vehicle. The goal is therefore to correctly size the hybrid electric/FC (powered by biomethane) waste collection vehicle so that it can perform the same mission as the traditional diesel vehicle [22].

In particular, the data required to properly describe the driving mission include: the speed profile (vehicle speed as a function of the elapsed time) obtained by GPS receiver, the electric current absorbed by the vehicle's electrical auxiliaries and the relative voltage, the flow rate and the hydraulic pressure necessary of the hydraulic auxiliaries (so hydraulic power can be calculated), and finally, it is necessary to know the vehicle weights at any moment of the speed profile to estimate the mass of the payload.

The speed profiles acquired via GPS signal need to be manually "cleaned". The "cleaning" of the profiles is carried out by deleting the data relating to those acquisition points where the GPS signal abruptly switched to speed values too high or too low (due to lack of signal).

The electrical power consumed by the vehicle's auxiliaries is calculated by multiplying the current by the voltage. The hydraulic power is instead obtained by multiplying the hydraulic flow by the pressure. Of the two powers absorbed by the vehicle auxiliaries, electric and hydraulic, the average over each speed profile is considered as an input parameter for the simulation. In particular, the sum of the two average powers will be set as input, as the total power consumed by the vehicle accessories.

The missions are carried out in flat territory; in fact, the altitude variation detected by the GPS is negligible. For the simulation, the complete absence of ground gradient is therefore imposed.

Table 1 shows the main characteristics of each of the 10 vehicle mission speed profiles.

Table 1. Main information of the speed profile of the waste collection vehicle mission.

Speed Profile n°	Distance Traveled [km]	Average Speed [km/h]	Profile Time [h:min:s]	Maximum Speed [km/h]	Average Electrical Power [W]	Average Hydraulic Power [W]	Total Power of the Auxiliaries [W]
1	34.707	8.8	3:56:31	86.4	540.9 *	215.6	756.5
2	39.361	8.3	4:42:59	55	442.6	174.6	617.2
3	43.570	9.0	4:51:34	62.5	671.6	73.3	744.9
4	13.780	13.6	10:07:08	108.7	531.2	131.5	662.7
5	81.789	16.1	5:04:55	105.5	561.5	241.0	802.5
6	50.003	9.0	5:32:58	75.1	566.9	247.2	814.1
7	72.137	12.4	5:47:39	83.3	597.3	202.6	799.9
8	60.671	14.7	4:07:42	85.7	540.9 *	303.6	844.5
9	89.048	16.1	5:31:43	106.6	498.7	267.7	766.4
10	85.977	19.5	4:24:27	92	457.6	255.3	712.9

* Electric power not available, estimated.

Regarding speed profile numbers 1 and 8, electric auxiliary power is not available due to sensor technical issues. In this case, the value is set equal to the average electrical power calculated on the other profiles (from 2 to 7, plus 9 and 10).

For each mission speed profile, the number of discharging cycles of the transported waste and the total weight unloaded are monitored (Table 2). Keeping in mind that dump is not always carried out in a landfill but is often carried out in intermediate areas discharging into a heavier vehicle (typically a truck), which then discharges at the landfill once full.

Table 2. Number of waste dumps and total weight unloaded for each mission speed profile.

Mission Profile n°	Types of Waste	Number of Unloads	Total Weight Unloaded [kg]	Average Weight Unloaded at Each Unloading [kg]
1	GLASS	1	1550	1550
2	ORGANIC WASTE	2	3000	1500
3	GENERAL WASTE	1	560	560
4	GLASS	2	1120	560
	YARD WASTE	1	400	400
	GENERAL WASTE	1	600	600
5	PLASTIC	7	900	128.57
6	PAPER	7	1700	242.86
7	ORGANIC WASTE	2	2680	1340
8	YARD WASTE	3	1250	416.67
	ORGANIC WASTE	2	2980	1490
9	ORGANIC WASTE	2	2720	1360
10	PLASTIC	4	650	162.5

Not having sufficient information available to define the entity of the waste mass transported by the vehicle instant by instant, it is decided to divide each speed profile into as many temporally equal parts as the unloads carried out and to distribute the unloaded weight equally for each dump (or for each group of unloads of the same type of waste,

as regards profiles 4 and 8). For each time interval between one unloading and the next, it is assumed that the transported waste mass grows linearly from the zero value to the average unloading value, as reported under the item "Average weight unloaded at each unloading [kg]" in Table 2 (Figure 2). A slightly different approach is used for profile 4: at time 14,191 s, the final unloading of the first group, consisting of two unloads, is carried out; it is therefore assumed to carry out the first unloading exactly halfway through the time elapsed before the second discharging (at 7095.5 s). The remaining time interval of the profile is equally divided among the other dumps. The approach adopted for the mass of the transported waste mass, on the other hand, remains unchanged compared to that adopted for the other profiles. Figure 2 shows the 10 speed profiles and the relative trend of the waste mass during the missions. In particular, the first 5 daily speed profiles are performed in a first week and the remaining 5 in a second week.

2.5. Simulation Tool

For the simulations of the vehicle and its missions, the TEST model described in Ref. [8] is used; in particular, the latest version of the model is used, the one containing the integration of the hydrogen FC [18] and its compressor, and the possibility to use a particular regenerative braking logic described in Ref. [17]. As it is not the target of this study, simulations are carried out with regenerative braking disabled.

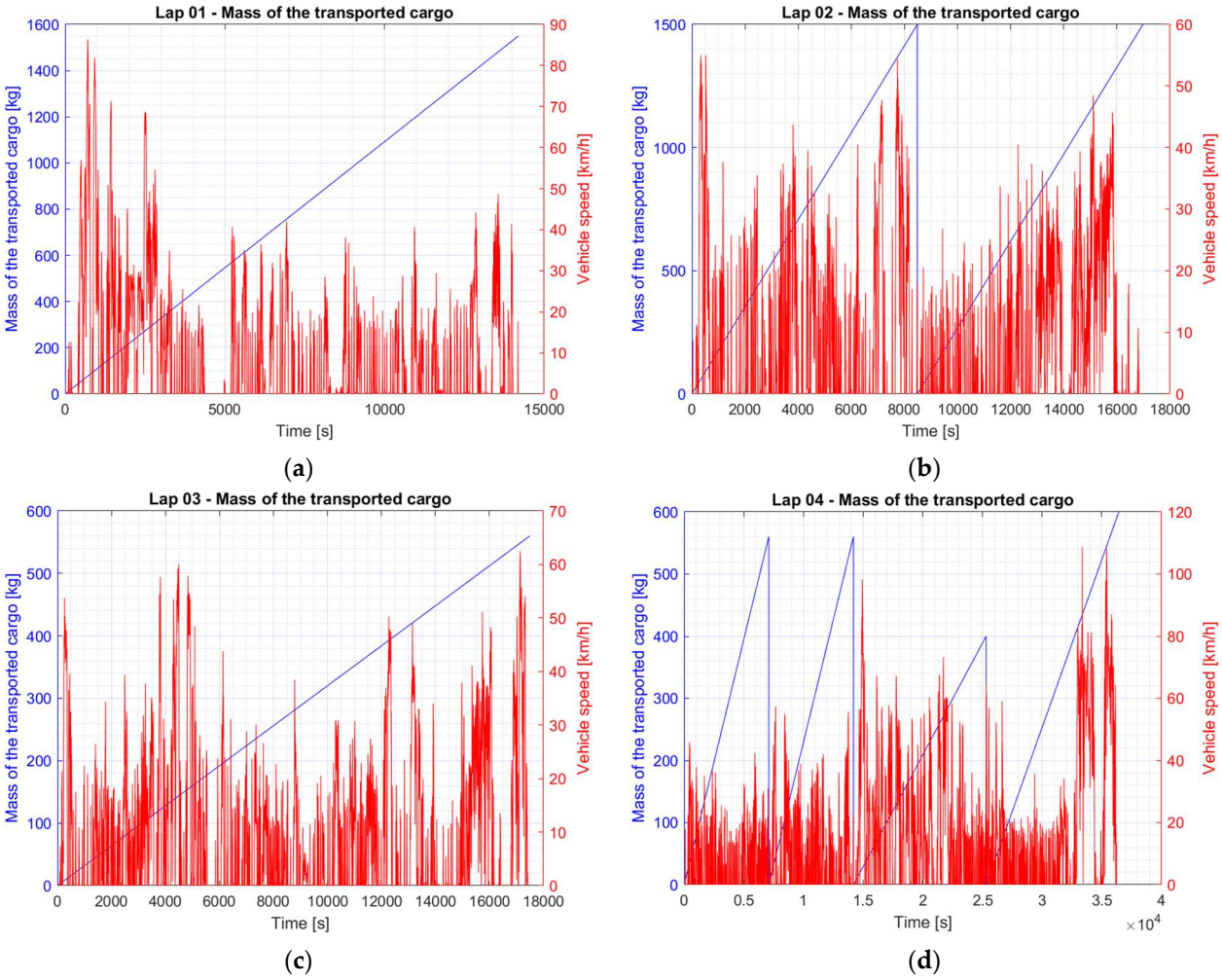

Figure 2. *Cont.*

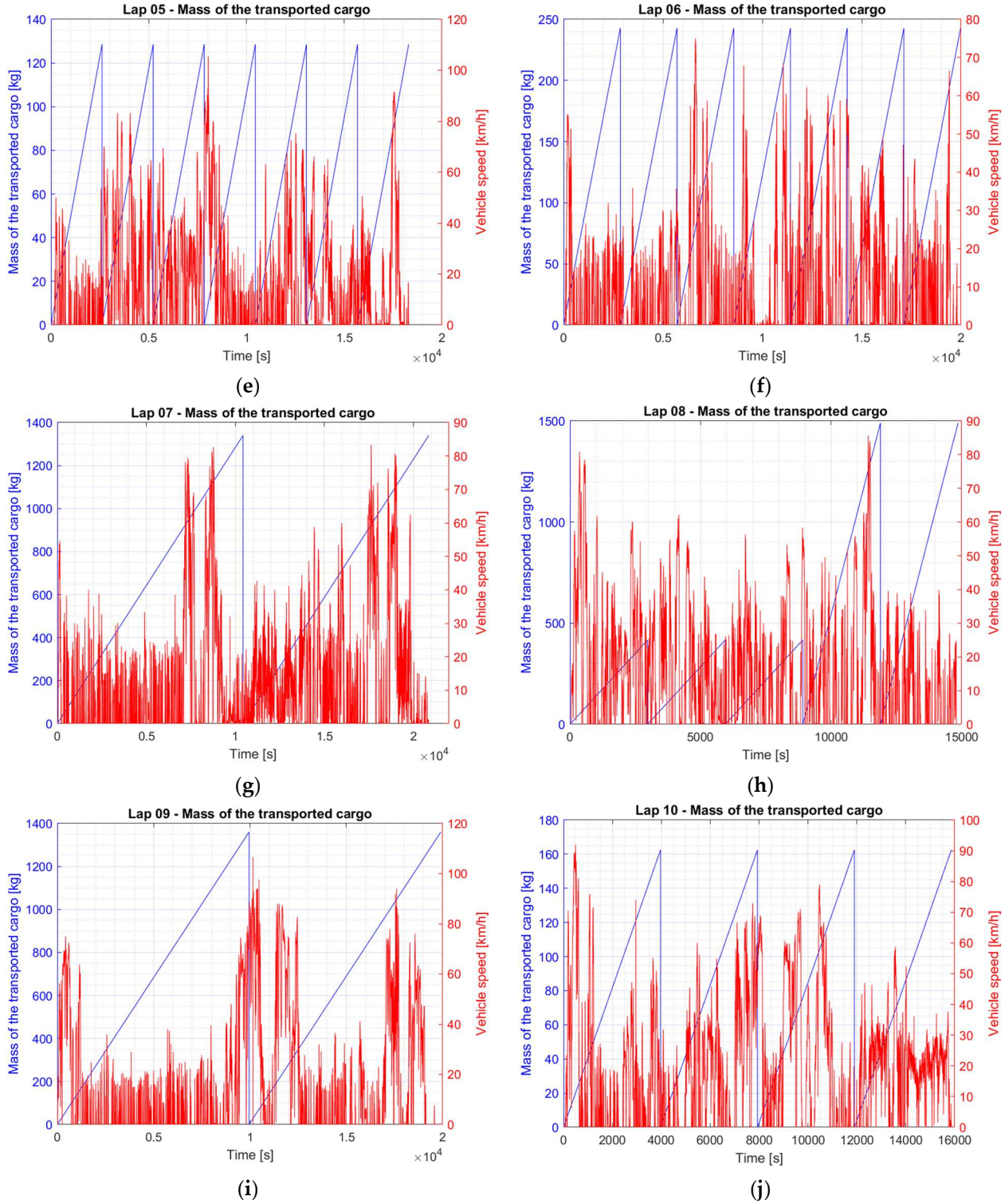

Figure 2. Carried loads (waste mass) and speed profiles of the missions: (**a**) profile 1; (**b**) profile 2; (**c**) profile 3; (**d**) profile 4; (**e**) profile 5; (**f**) profile 6; (**g**) profile 7; (**h**) profile 8; (**i**) profile 9; and (**j**) profile 10.

A modification is also made to the TEST model [8,17,18] that allows the user to input an additional variable mass according to the time elapsed from the start of the simulation, therefore, relating to the weight of the payload.

In particular, Equation (7) from Ref. [8] is rewritten as Equation (1).

$$F_\theta = \left(m_{vehicle} + m_{driver} + m_{fuel} + m_{cargo}\right) \cdot g \cdot \sin(\theta) \quad (1)$$

where F_θ is the additional resistance force given by the presence of the slope of the ground (θ), g is the gravity acceleration, $m_{vehicle}$ is the empty weight of the vehicle, m_{driver} is the driver's mass (plus the mass of any passengers), m_{fuel} is the mass of the fuel (considered constant during the simulation in this version of the model), necessary for powering any generators, and finally m_{cargo} is the mass of the payload carried by the vehicle given as a function of the time.

Equation (8) from Ref. [8] is rewritten as follows, in Equation (2), which also makes it possible to take into account the variation in rolling resistance as a function of vehicle speed.

$$F_r = \left[\left(m_{vehicle} + m_{driver} + m_{fuel} + m_{cargo}\right) \cdot g + \frac{1}{2} \cdot WHF \cdot \rho \cdot {v_{ref}}^2\right] \cdot f \cdot \cos(\theta) \quad (2)$$

where F_r is the rolling resistance, v_{ref} is the vehicle speed defined by the speed profile given as input data, WHF is the vertical aerodynamic coefficient, ρ is the air density, and f is the rolling resistance coefficient (See Equation (3)). In particular, Equation (3) predicts the values of f with acceptable accuracy for speeds up to approximately 130 km/h, as mentioned in Ref. [23].

$$f = f_r \cdot \left(1 + v_{ref} \cdot f_{r\_2}\right) \quad (3)$$

where f_r is the static rolling resistance coefficient, and f_{r_2} is the coefficient which allows to consider the rolling resistance coefficient as a linear function of speed.

Equation (10) from Ref. [8] is therefore rewritten as follows in Equation (4).

$$F_{tr} = a_{ref} \cdot \left(m_{vehicle} + m_{driver} + m_{fuel} + m_{cargo}\right) + F_{aero} + F_r + F_\theta \quad (4)$$

where F_{tr} is the traction force required (imposed by the speed profile given as input data), and F_{aero} is the aerodynamic resistance related to the speed profile.

Equation (40) from Ref. [8] is rewritten as Equation (5).

$$a = \frac{F_{tr\_F} + F_{tr\_R} - F_{wheels\_inertia\_F} - F_{wheels\_inertia\_R} - F_{brake} - F_d - F_r - F_\theta}{m_{vehicle} + m_{driver} + m_{fuel} + m_{cargo}} \quad (5)$$

where a is the calculated acceleration of the vehicle, F_{tr_F} and F_{tr_R} are the traction force provided by the front and rear motor, respectively, $F_{wheels\_inertia\_F}$ and $F_{wheels\_inertia\_R}$ are the inertia force of the front and rear wheels, respectively, F_{brake} is the ground force given by the hydraulic braking system, and F_d is the aerodynamic resistance related to the actual vehicle speed during the simulation.

Finally, Equation (47) from Ref. [8] is rewritten as Equation (6).

$$F_{brake\_req} = F_{tr\_F} + F_{tr\_R} - F_{aero} - F_r - F_\theta - \left(m_{vehicle} + m_{driver} + m_{fuel} + m_{cargo}\right) \cdot a_{ref} \quad (6)$$

where a_{ref} is the vehicle acceleration related to the speed profile given as input data.

Adding a new subsystem (called "SOFC peak power source"), a further integration is also made to this latest version of the TEST model, which allows it to also simulate vehicles equipped with a Solid Oxide Fuel Cell (SOFC) stack, which acts as a generator to charge the battery pack.

This subsystem outputs the power (P_{SOFC_th}) that the SOFC system can supply to the battery pack. In the first version of the TEST model, presented in paper [8], there was already a generator, or more generators, that can be activated to charge the batteries. The power that the generator, or generators, can supply as input to the battery pack, as

explained in Ref. [8], is defined with the variable P_{gen_th}, which is then supplied as input to the "Battery Limitations" module shown in Figure 1 in Ref. [8]. If the SOFC is present on the vehicle (activated by means of an appropriate switch presented later, Figure 3), the output power from the "SOFC peak power source" subsystem (P_{SOFC_th}) is assigned to the variable P_{gen_th}, through a Simulink "Switch", which allows to switch between the power of the generator(s) and the power coming from the SOFC, depending on which one is present on the vehicle. The rest of the calculation flow of the TEST model remains unchanged from previous versions.

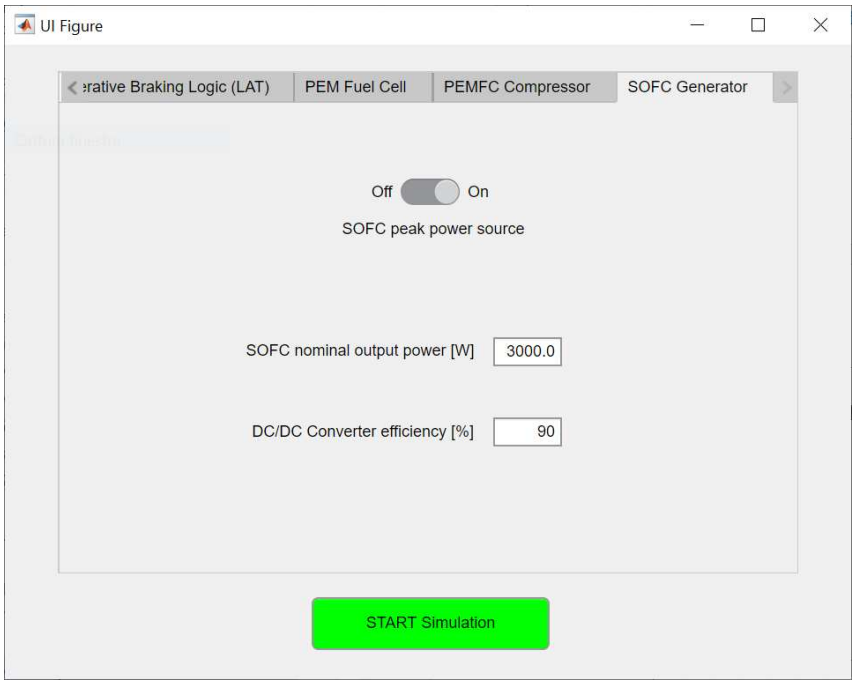

Figure 3. "SOFC Generator" panel of the Graphic User Interface of the TEST model [8,17,18]. In particular, this panel allows you to enter the inputs regarding the SOFC system.

For this study, the SOFC is seen as a sort of "black box"; only the constant power supplied by the FC (P_{SOFC}) and an efficiency relating to the DC/DC converter ($\eta_{DC/DC}$) are considered. DC/DC converter is in fact essential to carry the SOFC output voltage at the correct voltage for charging the battery pack. The calculation carried out within the "SOFC peak power source" module is therefore reduced to Equation (7) alone.

$$P_{SOFC\_th} = P_{SOFC} \cdot \eta_{DC/DC} \tag{7}$$

Finally, a further tab is added in the Graphic User Interface of the TEST model, relating to the definition of the variables P_{SOFC} and $\eta_{DC/DC}$, in which there is also a switch that allows you to activate ("On") or deactivate ("Off") the Solid Oxide Fuel Cell system (Figure 3).

Simulation Input Data

Below all the input values to be set in the TEST model will be shown [8,17,18], updated with the modifications shown in Section 2.5, for the simulations covered by the work presented in this paper. The name used for the variables refers to what is described in Ref. [8]. For simplicity, most of the input data used for the simulations will be shown through the graphical user interface panels of the TEST model [8] (Section 3).

As for the main simulation data:

- The relative speed profile, presented in Section 2.4, is used for each speed profile;

- Each profile is filtered using the parameter $k = 30$ (corresponding to a moving average of 30 samples);
- The battery pack temperature is set constant, and equal to 23 °C, for each speed profile;
- The elevation profile is defined constant and null for each speed profile;
- For all simulations, a "Sample Time" (t_s) equal to 0.05 s is used, which corresponds to the sampling interval of the GPS signal for each speed profile;
- The initial State of Charge of the battery pack, for each speed profile, is subject to sizing.

The vehicle being simulated is the door-to-door waste collection vehicle presented in Ref. [8] (Section 4.1), updated with some minor modifications and with the addition of the SOFC system on board (see Section 2.3). As seen in Ref. [8] (Section 4.1), this vehicle does not require any calibration regarding the mechanical part of the TEST model.

Below, common parameters to all simulations are reported (for all speed profiles).

- Air density: $\rho = 1.225\ \mathrm{kg/m^3}$;
- Gravity acceleration: $g = 9.81\ \mathrm{m/s^2}$;
- Electrical resistivity of conductor cables (copper): $\rho_{Cu} = 1.225\ \frac{\Omega \cdot \mathrm{mm}^2}{\mathrm{m}}$;
- Driver's weight (and no passengers): $m_{driver} = 80$ kg;
- Mass of fuel transported: $m_{fuel} = 0$. (The weight of the transported biomethane is already included in the weight of the SOFC system and already considered in the empty weight of the vehicle.)

It is worth to remember that the payload is set as defined in Section 2.4.

Using the tab shown in Figure 4, the inputs relating to the vehicle and the wheels are set, and the values shown in the above-mentioned figure are those used for all the simulations. The only exception is represented by the value of the total power consumed by the vehicle's auxiliaries, which relates only to speed profile number 7.

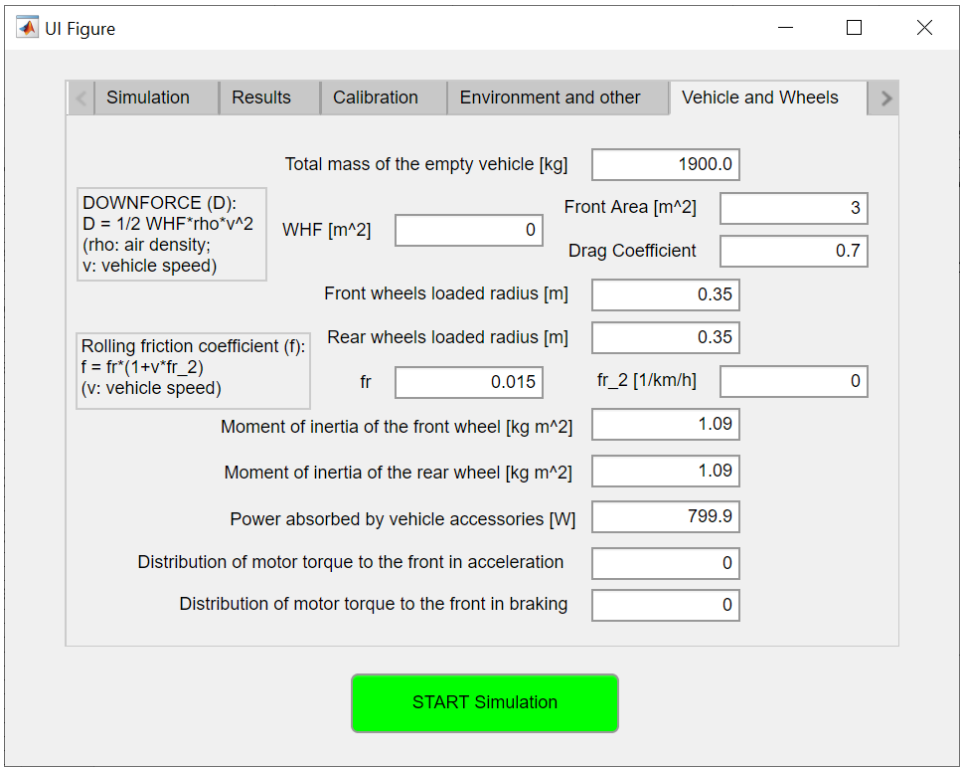

Figure 4. "Vehicle and Wheels" panel of the Graphic User Interface of the TEST model [8,17,18]. In particular, the panel in the figure shows the values adopted for the simulations of the waste collection vehicle equipped with SOFCs, relating to the vehicle in general and to the wheels. The only exception is represented by the value of the total power consumed by the vehicle's auxiliaries, which relates only to speed profile number 7.

The values of the total power consumed by the vehicle auxiliaries, for each speed profile, are those indicated under the item "Total power of the auxiliaries [W]" in Table 1.

Figure 5 shows the values of all the parameters relating to the vehicle's hydraulic braking system, used for all simulations.

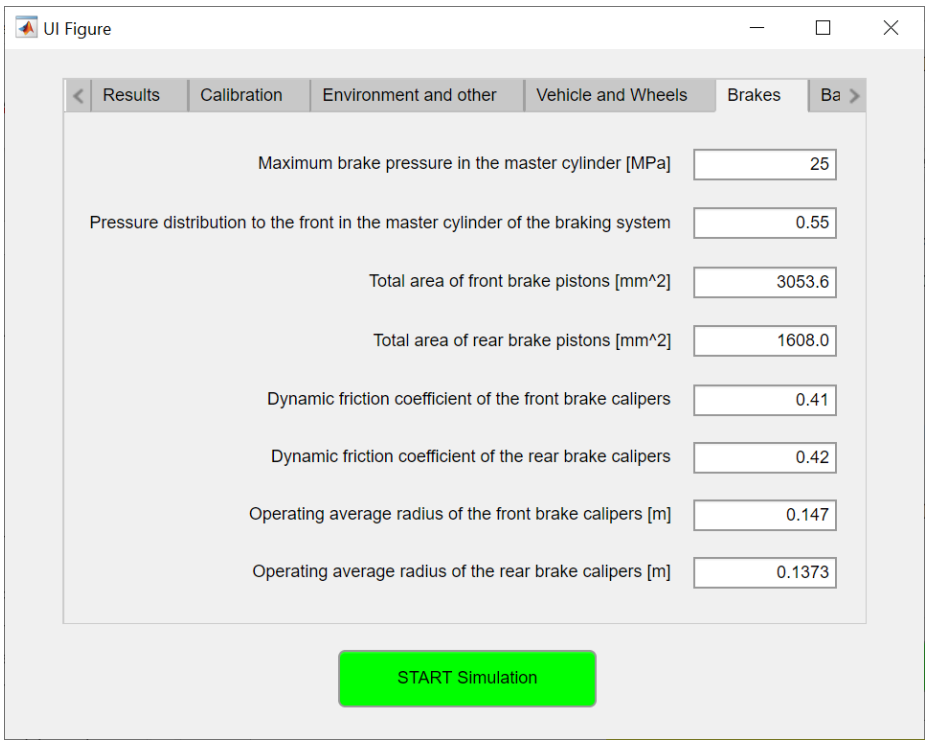

Figure 5. "Brakes" panel of the Graphic User Interface. In particular, the panel in the figure shows the values adopted for the simulations of the waste collection vehicle equipped with SOFCs, relating to the hydraulic braking system.

Concerning the battery pack, its capacity and rated power are chosen as reported in Section 2.6.

The following performances are set for the inverter that connects the battery pack and the motor.

- Inverter efficiency in the discharge phase of the battery pack: $\eta_{inv\_disch} = 0.88$;
- Inverter efficiency in the charge phase of the battery pack: $\eta_{inv\_ch} = 0.8$.

The vehicle is rear-wheel drive, so in the interface of the TEST model [8,17,18], the front electric motor is set to "Off" using the relative switch. Figure 6 shows the various parameters set for the simulations, inherent in the electric traction motor (which acts on the rear axle).

The motor torque curve of the vehicle being simulated is shown in Ref. [8] (Figure 5). Indeed, an efficiency map is included as well.

On board the vehicle, the only power generation is given by means of the SOFC; therefore, in the "Generators" panel of Ref. [8] (Figure 4g), a number of generators equal to zero is set.

Obviously, the switch of the panel relating to the SOFC generator (Figure 3) is set to "On" to activate the Solid Oxide Fuel Cell system which acts as a generator. The efficiency of the DC/DC converter that connects SOFCs and battery pack is estimated to be 90%, in accordance with what is reported in the literature [24,25]. The power supplied by the FC is sized according to the following section.

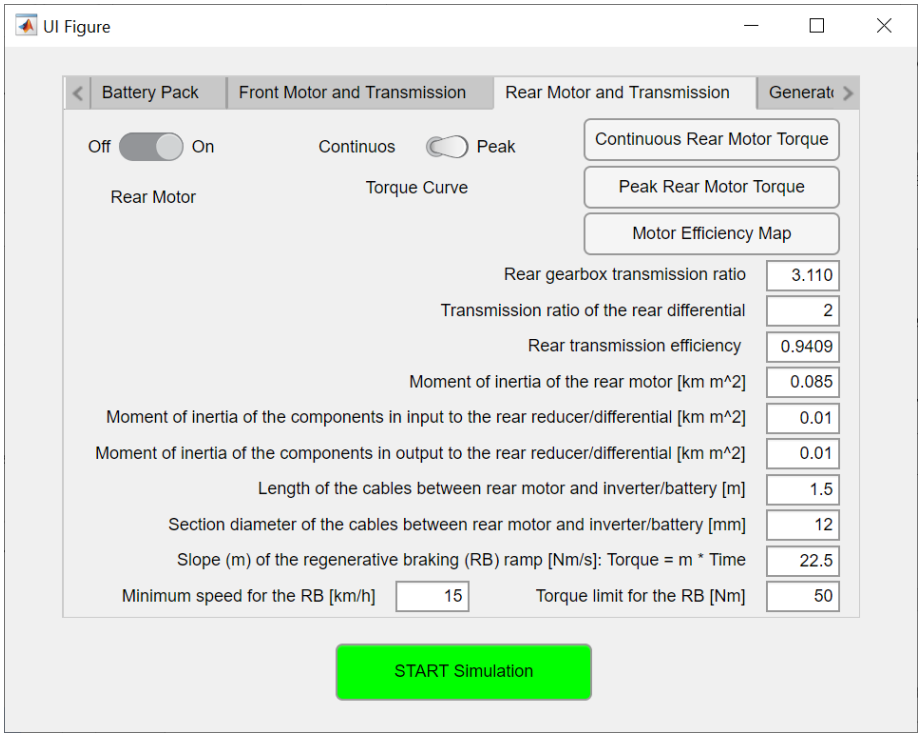

Figure 6. "Rear Motor and Transmission" panel of the Graphic User Interface. In particular, the panel in the figure shows the values adopted for the simulations of the waste collection vehicle equipped with SOFCs, relating to the electric motor.

2.6. Sizing of SOFCs and Battery Pack

First of all, an energy-oriented analysis of all the available speed profiles is carried out. Speed profile number 9 results to be associated with the greatest SOC decrease, and this is therefore the most expensive in terms of energy, followed by number 4 which is the most time-consuming, with about 10 h of profile time (See Table 1). It is therefore chosen to size the SOFC and the battery pack on profile 4, the longest in terms of time, so that it can be completed without stopping.

The sizing aims to obtain the following conditions:

- The system must be sized on the profile of about 10 h (profile 4), in such a way as to be able to carry out this profile during the day without any stopping;
- The battery pack size must be as small as possible (with the lowest possible capacity);
- The SOFC size must be as small as possible (lowest possible power rating);
- During the speed profiles, the battery pack must never reach an SOC of 100% (or get too close to it), to avoid having to implement the emergency condition of switching off the Fuel Cell;
- The battery pack must never drop below a minimum SOC (defined as 20%) that can lead to a lack of energy necessary to complete the speed profile and to a degradation of the battery pack itself;
- The sizing on profile 4 must be carried out in such a way as to exploit as much SOC field as possible, to ensure that the capacity of the battery pack and the power supplied by the SOFC are minimized;
- For the most energy-consuming profile (profile 9), a charging stop must be set at about mid-profile, as sizing components on speed profile number 4 makes it impossible to complete profile number 9 without stopping.

After an iterative process, consisted in carrying out simulations for profile 4 with different capacities of the battery pack and with different SOFC power ratings, the best compromise for battery pack size and SOFC power rating is found as:

- Battery pack capacity: 30 Ah;
- SOFC power rating: 3 kW.

These values, for speed profile number 4, allow us to exploit an SOC range between a maximum of 95.6% and a minimum of 20.6%, starting the profile with an initial SOC equal to 90% and ending it with a residual SOC equal to 21.3%.

As mentioned above, the vehicle with a 3 kW SOFC and a 30 Ah battery pack is unable to complete mission number 9 without stopping. The profile is therefore divided approximately in half (with respect to time) to plan an intermediate stop (with the vehicle switched off), during which the battery pack is charged by the SOFC. In this case, it is worth to remember that the SOFC is supposed to stay active for the entire life of the vehicle. The speed profile number 9 is therefore split into two, as shown in Figure 7 (profile 9.a and profile 9.b). By overlaying the GPS data in Google Earth, the presence of a waste unload point at 9150 s elapsed time from the start of the profile is noted. Subsequently, the vehicle moves empty for a certain time, without making any collections, to change the collection area. According to these hypotheses, the estimated and approximate trends of the mass of the transported waste load are constructed as a function of the simulation time, as reported in Figure 7.

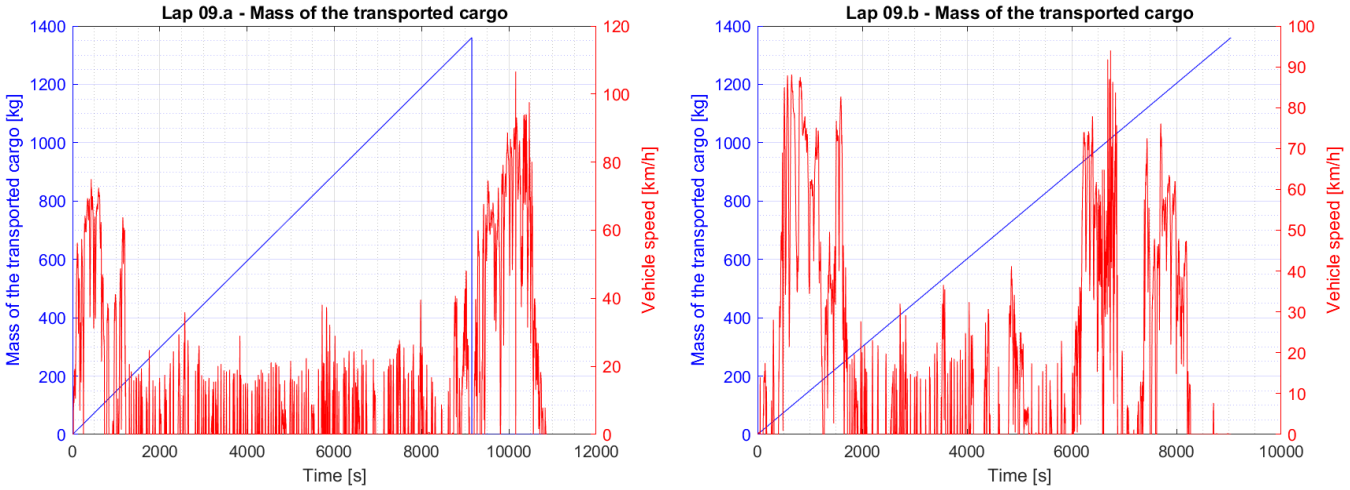

(**a**) (**b**)

Figure 7. Carried waste load and speed profile of the mission: (**a**) first phase of profile 9 (profile 9.a); (**b**) second phase of profile 9 (profile 9.b).

Finally, for the simulations of both profiles (profile 9.a and profile 9.b), the total power consumed by all vehicle auxiliaries is considered the average calculated on the entire speed profile number 9 (shown in Table 1).

From the simulations, it is found that a charging stop of an hour and a half is enough to complete the mission without any further stop.

3. Results

Figure 8 shows the simulation results in terms of battery State of Charge (SOC) and vehicle speed, for each door-to-door waste collection mission.

As can be seen from Figure 8, the low energy-demanding maneuvers, such as low accelerations or stops to collect waste, are associated with an SOC increase because the power demand is lower than the power delivered by the SOFCs.

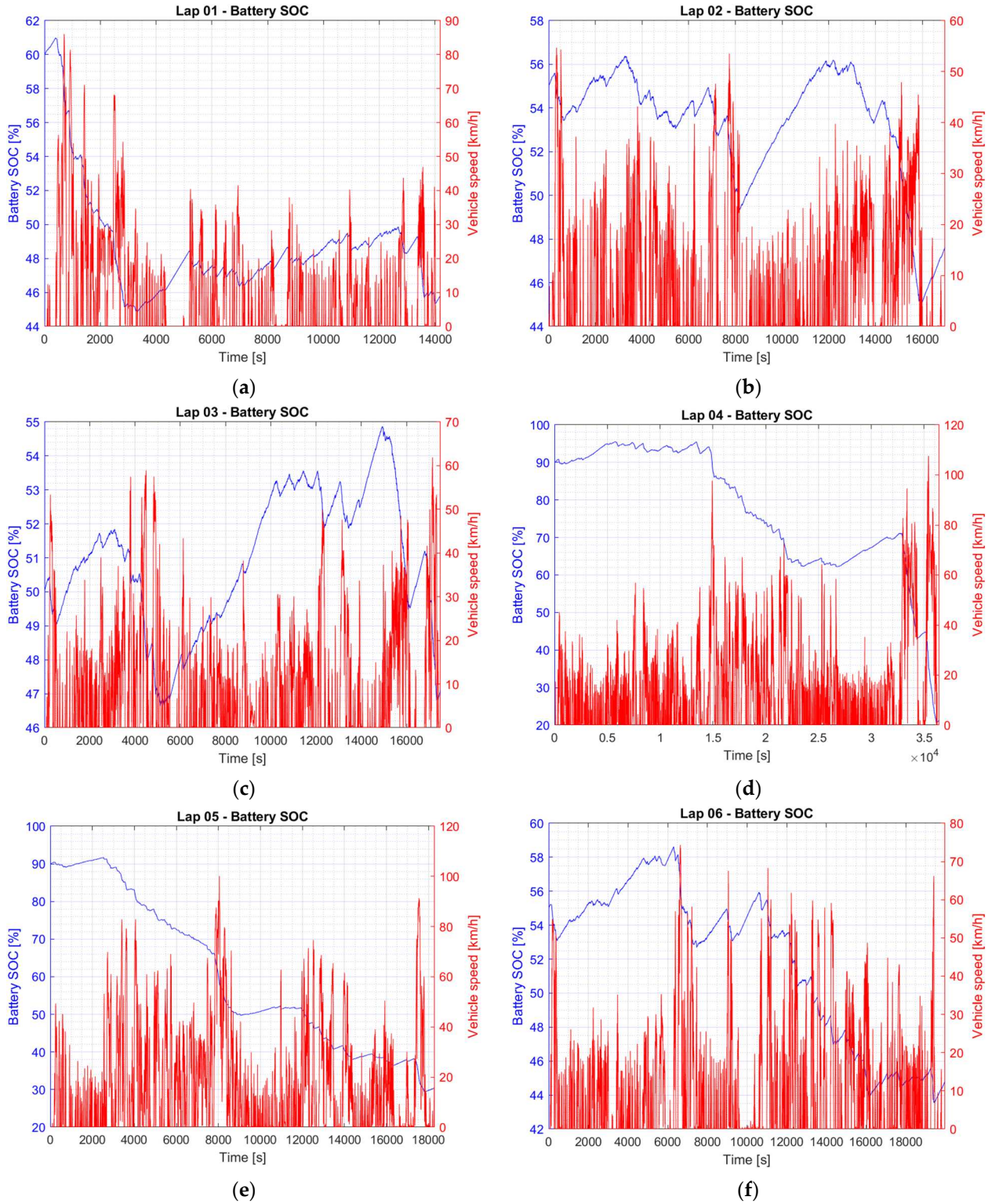

Figure 8. *Cont.*

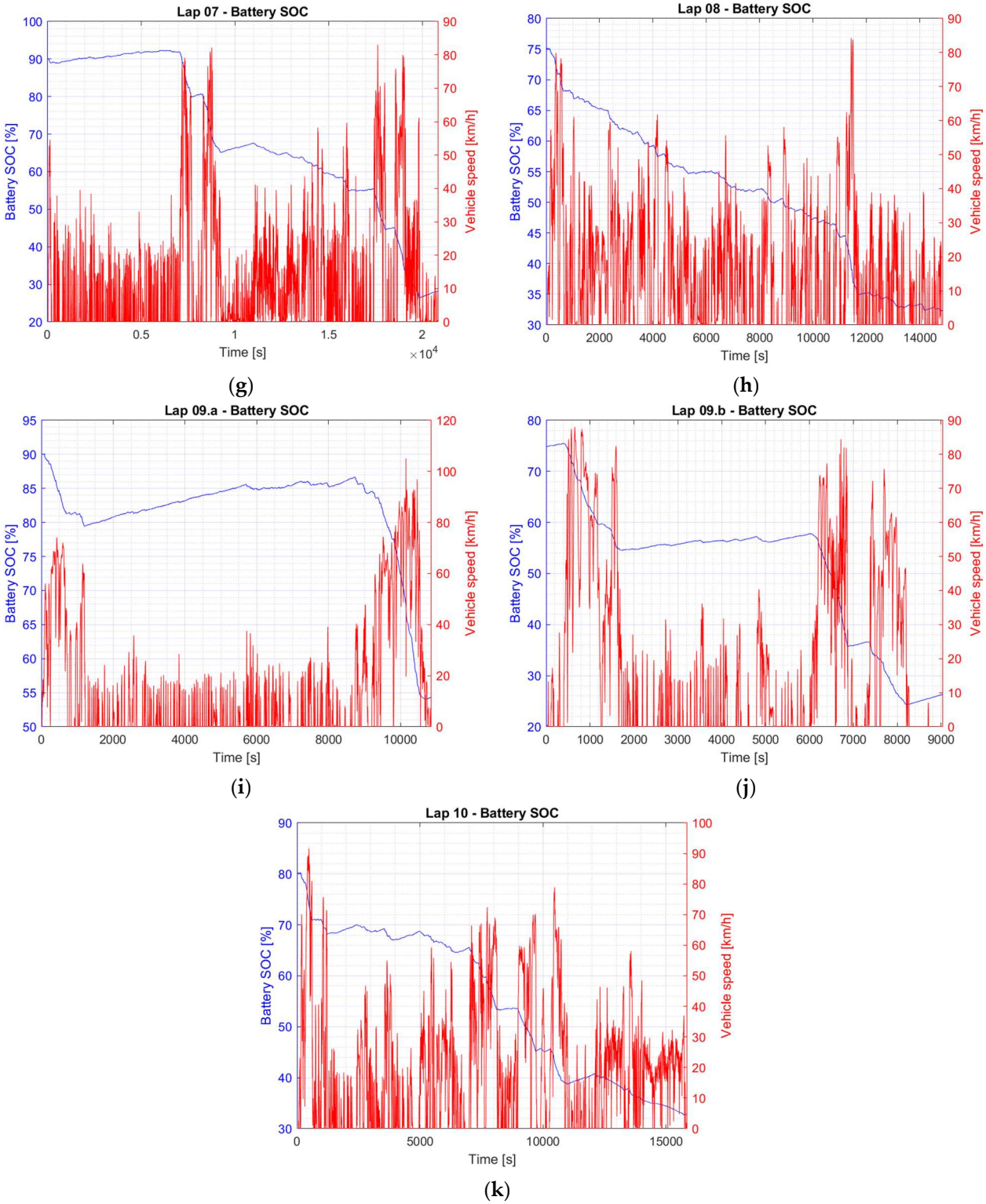

Figure 8. Battery State of Charge (SOC) and speed profile of the mission for the TEST simulation on: (**a**) profile 1; (**b**) profile 2; (**c**) profile 3; (**d**) profile 4; (**e**) profile 5; (**f**) profile 6; (**g**) profile 7; (**h**) profile 8; (**i**) profile 9.a; (**j**) profile 9.b; and (**k**) profile 10.

Table 3 summarizes the main results obtained for the vehicle model with an SOFC generator that supplies a constant power equal to 3 kW and has a 30 Ah capacity battery pack.

Table 3. Main results of the speed profiles of the mission of the waste collection vehicle equipped with SOFCs. In particular, the item "SOC range [%]" refers to the portion of SOC used during the journey of the mission profile. It is therefore calculated as the difference between the maximum SOC and the minimum SOC reached during the profile during the exam.

Speed Profile n°	Initial SOC [%]	Final SOC [%]	Maximum SOC [%]	Minimum SOC [%]	SOC Range [%]	Profile Time [h:min:s]	Charging Time [h:min:s]
1	60 *	45.7	61.0	44.8	16.1	3:56:31	1:02:45
2	55 *	47.6	56.4	45.1	11.3	4:42:59	0:32:25
3	50 *	47.1	54.9	46.6	8.2	4:51:34	0:12:44
4	90 *	21.3	95.6	20.6	74.9	10:07:08	5:02:09
5	90 *	30.4	91.7	29.5	62.2	5:04:55	4:22:07
6	55 *	44.8	58.6	43.5	15.1	5:32:58	0:44:50
7	90 *	28.3	92.3	26.4	66.0	5:47:39	4:31:14
8	75 *	32.4	75.1	32.2	42.9	4:07:42	3:07:13
9.a	90 *	54.4	90.1	54.1	36.0	3:01:02	1:30:00 *
9.b	74.8	26.3	75.5	24.4	51.1	2:30:41	4:39:57
10	80 *	32.9	80.2	32.7	47.6	4:24:27	3:27:05

* Quantity subject to sizing.

The speed profiles from numbers 1 to 10 are daily profiles, to be carried out over two weeks (each profile only once every two weeks). The two-week mission is then repeated continuously throughout the year without weeks of stop. Each profile must be carried out starting with an initial SOC equal to the value reported under the heading "Initial SOC [%]" in Table 3. Therefore, the residual SOC (final SOC) of the profile preceding the one considered must be reported on the initial value of the new daily profile to be carried out on the following working day. Considering that the final SOC of each profile is lower than its initial SOC, the sum of all the charging phases between one profile and the next corresponds to the sum of all the charging phases necessary to bring the final SOC of a profile back to the initial SOC of the profile itself. This aspect greatly simplifies the problem; in fact, to obtain the total charge time between the various speed profiles, it is enough to associate the value reported under the item "Charging time [h:min:s]" in Table 3 to each speed profile. This value corresponds precisely to the time needed to charge the battery pack from the final SOC of the considered profile to the initial SOC of the profile itself, with the vehicle off (and SOFCs always on). However, it is worth highlighting that the charge time associated with profile 9.a corresponds to the partial charge time of an hour and a half sized in order to be able to complete profile 9.b. The charge time associated with profile 9.b is instead the time required to charge the battery pack from the final SOC of profile 9.b to the initial SOC of profile 9 and then to the initial SOC of profile 9.a.

Therefore, by adding all the charging times associated with each speed profile, an overall charging time of 29 h, 12 min, and 29 s is obtained every two weeks of vehicle operation. The total profile time is instead given by the sum of all the values reported under the item "Profile time [h:min:s]" in Table 3 and corresponds to a total of 54 h, 7 min, and 34 s, in which the vehicle is operational within a two-week timespan.

The total time, every two weeks, in which the SOFC operates to supply energy for the speed profiles, corresponds to the sum of the total time spent on the profiles and the total charge time. It therefore corresponds to 83 h, 20 min, and 3 s.

Considering that two weeks have a total of 336 h, subtracting from this the time in which the SOFC operates to provide energy for the mission, in the remaining 252 h, 39 min, and 57 s, the SOFC will supply power to the electrical grid. Therefore, for approximately 253 h, the vehicle must be connected to the stationary electricity grid or, alternatively, to other infrastructure with similar functionality (infrastructure for charging other vehicles in the fleet, for example, full electric vehicles, charging infrastructure for a stationary energy storage system, etc.).

Considering an SOFC methane consumption equal to 0.23 m^3 h^{-1} kW^{-1}, according to Ref. [26], the 3 kW SOFC stack leads to a fuel consumption of 0.69 m^3 h^{-1}. Hence, the amount of methane needed to power the vehicle over the two-week timespan can be calculated. Every two weeks, 57.5 m^3 of methane is needed to ensure the traction of the vehicle; in particular, 37.3 m^3 of methane is consumed during the vehicle operation (with the vehicle on), running through the speed profiles of the mission, while 20.2 m^3 is consumed during the battery pack recharging phases (with the vehicle off), considering that the SOFC system always remains on for the entire life of the vehicle. Thus, every two weeks, the vehicle consumes 231.8 m^3 of methane. By subtracting from the latter, the amount of methane required to guarantee traction, it was found that 174.3 m^3 will be used to send power into the grid (or charge other electric vehicles). Table 4 summarizes the above-discussed results.

Table 4. Methane consumption every two weeks for each phase of the vehicle's life.

Total	Phase	Sub-Phase
Every two weeks 231.8 m^3	Traction, for recharging the battery pack 57.5 m^3	During vehicle's mission (vehicle on) 37.3 m^3
		During recharge phases (vehicle off) 20.2 m^3
	Vehicle off, for recharging the electricity grid 174.3 m^3	

4. Discussion

The aim of this study was to investigate the possibility to employ an FC-powered hybrid fueled by biomethane (or methane). This was conducted through a model-based design approach, using a consolidated vehicle modeling architecture/tool [8,17,18]. Concerning the Fuel Cell itself, the chemistry identified is the so-called SOFCs (Solid Oxide Fuel Cells), which allows (by means of its internal reforming process) to be fed with fuels other than hydrogen, including methane. However, the SOFCs are limited by different problems, in particular, by a high structural fragility (to be solved before the installation of the latter on a moving vehicle), long ignition times, and slow transients. The SOFC vehicle model that was created and integrated into the TEST model [8,17,18] is a vehicle that operates in a fleet operating as door-to-door waste collection, with a predefined driving mission. Furthermore, the vehicle simulated has a series hybrid electric layout, with an electric motor powered by a battery pack (acting as peak power source) and an SOFC system delivering constant power. Because of its very long start-up and transient times, the SOFC is supposed to be always operative, even when the vehicle is not carrying out its mission. When the vehicle is not in operation and the battery pack does not need to be charged, the vehicle must be connected to the electricity grid and the SOFCs will supply power to it. Alternatively, it is possible to charge the battery pack of other electric vehicles in the fleet or to charge a stationary energy storage system. In other words, this vehicle can be seen as a mobile power station itself.

Finally, through the example of the waste collection vehicle, the methodology to be adopted for the construction of a hybrid electric/SOFC vehicle was shown.

The work carried out is therefore repeatable and can be the basis for future works aimed at exploiting Solid Oxide Fuel Cell technology in the automotive sector. This can in fact be useful to solve the range problems associated with full electric vehicles and to exploit a methane alimentation, of which infrastructure is already available. Furthermore, by feeding the SOFCs with biomethane, it is possible to exploit a renewable energy source with theoretically net-zero environmental impact (considering the entire life cycle of the biomethane itself).

The impact on air quality and GHG emissions of a commercial vehicle fleet equipped with Solid Oxide Fuel Cells can be assessed using integrated assessment models. In particular, starting from the data obtained in this work, it is possible to define an environmental assessment of the introduction of these SOFC hybrid technologies in the commercial vehicle fleet. The study could calculate the total emissions reduction due to the partial replacement of the traditional light-duty vehicle fleet with vehicles equipped with SOFC powertrain and then estimate the air quality impact using an integrated assessment model, such as MAQ (Multi-dimensional Air Quality) [27].

5. Conclusions

By means of the analysis of the literature and the study on the operation of Solid Oxide Fuel Cells, it was possible to lay the foundations and initial hypotheses for the construction of a hybrid electric/SOFC vehicle model.

This led to the choosing of a series hybrid electric vehicle layout with an electric motor powered by a battery pack (acting as peak power source) and an SOFC system delivering constant power to solve the problem of slow transients of the SOFCs. Furthermore, the extreme hypothesis of a Fuel Cell system being always on and of a vehicle connected to the electricity grid during the inactivity phases was carried out to solve the problem of the long start-up times of the SOFCs. This vehicle layout is therefore suitable to be used for vehicles operating in a fleet with predefined missions. The components of the system, such as the battery pack and the SOFCs, must be suitably sized in such a way as to guarantee the functionality of the vehicle and allow for the meeting of the requirements of the mission. In particular, a 30 Ah battery pack and a 3 kW SOFC system were chosen for the purpose of this work.

In this paper, a door-to-door waste collection vehicle was considered, which operates in a fleet on predefined daily waste collection missions. Based on the mission data, it was possible to size the vehicle's components and establish the pre-set conditions to which the various speed profiles will have to undergo during operation (in particular, the initial SOC of the profile of each daily mission).

Therefore, starting from the creation of a model for a particular vehicle (the waste collection vehicle), it was possible to show the methodology to be adopted for the sizing and construction of a model of a generic SOFC vehicle that operates in fleet. The work conducted is therefore repeatable and can also be adapted to other types of vehicles, making sure to pay attention to the fact that there is a need for a predefined and fixed mission over a certain period (for example, the two-week timespan of the waste collection vehicle).

Furthermore, it is necessary to solve the problems of the fragility and low resistance of the Solid Oxide Fuel Cells before their installation on board a real vehicle. After that, it will be possible to use the SOFC technology for fleet vehicles with predefined missions.

Finally, the battery has a limited number of cycles. The results obtained from this study can be used to determine the battery's expiration date, but this requires battery data that are difficult to find. Therefore, at this stage, this aspect was left out, and it may still represent a possible future development.

Author Contributions: Conceptualization, G.S., M.G., D.C. and L.Z.; methodology, G.S.; software, G.S.; data curation, G.S.; writing—original draft preparation, G.S., M.G., D.C. and L.Z.; writing—review and editing, G.S., M.G., D.C. and L.Z.; visualization, M.G. and D.C.; supervision, M.G. and D.C. All authors have read and agreed to the published version of the manuscript.

Funding: This work was supported in part by the Hub Biomass Project [ID 1165247, PORFESR 2014–2020, and Regione Lombardia (IT)].

Data Availability Statement: The data presented in this study are available on request from the corresponding author. The data are not publicly available due to University of Brescia privacy policy.

Acknowledgments: Acknowledgement goes to Andrea Tonola (Department of Mechanical and Industrial Engineering, University of Brescia) for collaborating in the search for information regarding Solid Oxide Fuel Cell technology.

Conflicts of Interest: The authors declare no conflict of interest.

Abbreviation

Abbreviation	Description
a	Longitudinal vehicle acceleration [2]
a_{ref}	Reference vehicle acceleration [3,4]
CO_2	Carbon dioxide
DC	Direct Current
FC	Fuel Cell
f	Rolling resistance coefficient [2]
F_{aero}	Aerodynamic resistance, drag (calculated in the TEST model, using vehicle speed of the previous instant of calculation) [3]
F_{brake}	Force given by the traditional hydraulic brakes [3]
F_{brake_req}	Force required to traditional hydraulic brakes [3]
F_d	Aerodynamic resistance, drag [2]
F_r	Rolling resistance [2]
f_r	Static rolling resistance coefficient [1]
f_{r_2}	Coefficient which allows to consider the rolling resistance coefficient as a linear function of vehicle speed [1]
F_{tr}	Traction force [3]
F_{tr_F}	Portion of traction force which must be guaranteed by the front motor [3]
F_{tr_R}	Portion of traction force which must be guaranteed by the rear motor [3]
$F_{wheels\_inertia\_F}$	Force lost due to inertia of the front wheels ("forward-facing" approach, in the TEST model) [3]
$F_{wheels\_inertia\_R}$	Force lost due to inertia of the rear wheels ("forward-facing" approach, in the TEST model) [3]
F_θ	Additional force given by the presence of the slope of the ground [2]
g	Gravity acceleration [1]
GPS	Global Position System
k	Local k-point mean values for the moving mean of speed profile [1]
m_{cargo}	Mass of the transported cargo [1]
m_{driver}	Driver's mass (plus the mass of any passengers) [1]
m_{fuel}	Mass of the fuel [1]
$m_{vehicle}$	Unloaded mass of the vehicle [1]
PAFC	Phosphoric Acid Fuel Cell
PEFC	Polymer Electrolyte Fuel Cell
PEMFC	Proton Exchange Membrane Fuel Cell
P_{gen_th}	Total maximum power that the generators can supply as input to the battery pack [3]
P_{SOFC}	Charging power that the SOFC system sends to the battery pack [5]
P_{SOFC_th}	Constant power supplied by SOFCs [1,5]
SOC	Battery State of Charge
SOFC	Solid Oxide Fuel Cell
TEST	Target-speed EV Simulation Tool
t_s	Sampling time of the TEST simulation [1]
v_{ref}	Reference vehicle speed [4]
WHF	Vertical aerodynamic coefficient [1]
WLTC	Worldwide Harmonized Light-Duty Vehicles Test Cycle
WLTP	Worldwide Harmonized Light-Duty Vehicles Test Procedure
$\eta_{DC/DC}$	Efficiency of the SOFC DC/DC converter [1,5]
η_{inv_ch}	Efficiency of the inverter in charge [1]
η_{inv_disch}	Efficiency of the inverter in discharge [1]
θ	Road slope angle [4]
ρ	Air density [1]
ρ_{Cu}	Electric resistivity of copper (or in any case of the conductive material of the electric cables)

[1] Constant value. [2] Variable. [3] "TEST model" calculated variable. [4] "TEST model" input. [5] SOFC model.

References

1. Mellone, R. Il mondo delle SOFC, o Celle a Combustibile ad Ossidi Solidi (The world of SOFCs, or Solid Oxide Fuel Cells). 14 February 2020. Available online: https://energycue.it/mondo-sofc-celle-combustibile-ossidi-solidi/17825/ (accessed on 19 June 2023).
2. Krummrein, T.; Henke, M.; Kutne, P.; Aigner, M. Numerical Analysis of Operating Range and SOFC-off-Gas Combustor Requirements of a Biogas Powered SOFC-MGT Hybrid Power Plant. *Appl. Energy* **2018**, *232*, 598–606. [CrossRef]
3. Mangifesta, P. Semicelle Sofc: Studio e Produzione di Elettroliti Con Processi a Basso Impatto Ambientale. Ph.D. Thesis, Università degli Studi di Bologna—Facoltà di Chimica Industriale, Bologna, Italy, 2009.
4. Lu, Y.; Cai, Y.; Souamy, L.; Song, X.; Zhang, L.; Wang, J. Solid Oxide Fuel Cell Technology for Sustainable Development in China: An over-View. *Int. J. Hydrogen Energy* **2018**, *43*, 12870–12891. [CrossRef]
5. Lan, T.; Strunz, K. Multiphysics Transients Modeling of Solid Oxide Fuel Cells: Methodology of Circuit Equivalents and Use in EMTP-Type Power System Simulation. *IEEE Trans. Energy Convers.* **2017**, *32*, 1309–1321. [CrossRef]
6. Gür, T.M. Comprehensive Review of Methane Conversion in Solid Oxide Fuel Cells: Prospects for Efficient Electricity Generation from Natural Gas. *Prog. Energy Combust. Sci.* **2016**, *54*, 1–64. [CrossRef]
7. Ma, R.; Liu, C.; Bai, H.; Breaz, E.; Briois, P.; Gao, F. A Multi-Domain Syngas Solid Oxide Fuel Cell Model for Transportation Applications. In Proceedings of the 2018 IEEE International Conference on Industrial Electronics for Sustainable Energy Systems (IESES), Hamilton, New Zealand, 31 January–2 February 2018; pp. 189–194.
8. Sandrini, G.; Gadola, M.; Chindamo, D. Longitudinal Dynamics Simulation Tool for Hybrid Apu and Full Electric Vehicle. *Energies* **2021**, *14*, 1207. [CrossRef]
9. Chindamo, D.; Gadola, M.; Romano, M. Simulation Tool for Optimization and Performance Prediction of a Generic Hybrid Electric Series Powertrain. *Int. J. Automot. Technol.* **2014**, *15*, 135–144. [CrossRef]
10. Ma, S.; Lin, M.; Lin, T.-E.; Lan, T.; Liao, X.; Maréchal, F.; Van herle, J.; Yang, Y.; Dong, C.; Wang, L. Fuel Cell-Battery Hybrid Systems for Mobility and off-Grid Applications: A Review. *Renew. Sustain. Energy Rev.* **2021**, *135*, 110119. [CrossRef]
11. Lawlor, V.; Reissig, M.; Makinson, J.; Rechberger, J. SOFC System for Battery Electric Vehicle Range Extension: Results of the First Half of the Mestrex Project. *ECS Trans.* **2017**, *78*, 191–195. [CrossRef]
12. Rafikiran, S.; Basha, C.H.H.; Murali, M.; Fathima, F. Design and Performance Evaluation of Solid Oxide-Based Fuel Cell Stack for Electric Vehicle System with Modified Marine Predator Optimized Fuzzy Controller. *Mater. Today Proc.* **2022**, *60*, 1898–1904. [CrossRef]
13. Udomsilp, D.; Rechberger, J.; Neubauer, R.; Bischof, C.; Thaler, F.; Schafbauer, W.; Menzler, N.H.; de Haart, L.G.J.; Nenning, A.; Opitz, A.K.; et al. Metal-Supported Solid Oxide Fuel Cells with Exceptionally High Power Density for Range Extender Systems. *Cell Rep. Phys. Sci.* **2020**, *1*, 100072. [CrossRef]
14. Tanozzi, F.; Sharma, S.; Maréchal, F.; Desideri, U. 3D Design and Optimization of Heat Exchanger Network for Solid Oxide Fuel Cell-Gas Turbine in Hybrid Electric Vehicles. *Appl. Therm. Eng.* **2019**, *163*, 114310. [CrossRef]
15. Kerviel, A.; Pesyridis, A.; Mohammed, A.; Chalet, D. An Evaluation of Turbocharging and Supercharging Options for High-Efficiency Fuel Cell Electric Vehicles. *Appl. Sci.* **2018**, *8*, 2474. [CrossRef]
16. Commission Regulation (EU) 2017/1151. Available online: https://www.legislation.gov.uk/eur/2017/1151/contents (accessed on 19 June 2023).
17. Sandrini, G.; Chindamo, D.; Gadola, M. Regenerative Braking Logic That Maximizes Energy Recovery Ensuring the Vehicle Stability. *Energies* **2022**, *15*, 5846. [CrossRef]
18. Zecchi, L.; Sandrini, G.; Gadola, M.; Chindamo, D. Modeling of a Hybrid Fuel Cell Powertrain with Power Split Logic for Onboard Energy Management Using a Longitudinal Dynamics Simulation Tool. *Energies* **2022**, *15*, 6228. [CrossRef]
19. Ehsani, M.; Gao, Y.; Longo, S.; Ebrahimi, K. 15 Fuel Cells. In *Modern Electric, Hybrid Electric, and Fuel Cell Vehicles*; CRC Press; Taylor & Francis Group: Boca Raton, FL, USA, 2018; pp. 397–420.
20. Chen, G.; Luo, Y.; Sun, W.; Liu, H.; Ding, Y.; Li, Y.; Geng, S.; Yu, K.; Liu, G. Electrochemical Performance of a New Structured Low Temperature SOFC with BZY Electrolyte. *Int. J. Hydrogen Energy* **2018**, *43*, 12765–12772. [CrossRef]
21. 2022 MoTeC Pty Ltd. MoTeC—Products—Engine Management. Available online: https://www.motec.com.au/Main/ECUwizard/ (accessed on 3 November 2022).
22. Chindamo, D.; Gadola, M. What Is the Most Representative Standard Driving Cycle to Estimate Diesel Emissions of a Light Commercial Vehicle? *IFAC-PapersOnLine* **2018**, *51*, 73–78. [CrossRef]
23. Ehsani, M.; Gao, Y.; Longo, S.; Ebrahimi, K. 2 Fundamentals of Vehicle Propulsion and Braking. In *Modern Electric, Hybrid, and Fuel Cell Vehicles*; CRC Press; Taylor & Francis Group: Boca Raton, FL, USA, 2018; pp. 18–20.
24. Al, M.; Van, J.; Gualous, H. DC/DC Converters for Electric Vehicles. In *Electric Vehicles—Modelling and Simulations*; InTech: London, UK, 2011; Available online: https://www.intechopen.com/chapters/19583 (accessed on 19 June 2023).
25. Brett, D.J.L.; Aguiar, P.; Brandon, N.P.; Bull, R.N.; Galloway, R.C.; Hayes, G.W.; Lillie, K.; Mellors, C.; Smith, C.; Tilley, A.R. Concept and System Design for a ZEBRA Battery–Intermediate Temperature Solid Oxide Fuel Cell Hybrid Vehicle. *J. Power Sources* **2006**, *157*, 782–798. [CrossRef]

26. Aguiar, P.; Brett, D.J.L.; Brandon, N.P. Feasibility Study and Techno-Economic Analysis of an SOFC/Battery Hybrid System for Vehicle Applications. *J. Power Sources* **2007**, *171*, 186–197. [CrossRef]
27. Turrini, E.; Carnevale, C.; Finzi, G.; Volta, M. A Non-Linear Optimization Programming Model for Air Quality Planning Including Co-Benefits for GHG Emissions. *Sci. Total Environ.* **2018**, *621*, 980–989. [CrossRef] [PubMed]